Symmetry Breaking Instabilities of an *In Vitro* Biological System

Ken Sekimoto
Yukawa Institute for Theoretical Physics, Kyoto University, Kyoto 606-01, Japan

Naoki Mori
Department of Applied Physics, Nagoya University, Nagoya 464-01, Japan

Katsuhisa Tawada
Department of Biology, Faculty of Science, Kyushu University, Fukuoka 812, Japan

Yoko Y. Toyoshima
Department of Pure and Applied Sciences, College of Arts and Sciences, University of Tokyo, Tokyo 153, Japan
(Received 17 December 1994)

Spontaneous rotation and flapping oscillations of an actin filament driven by myosins have been observed in the *in vitro* setup of a quasi-two-dimensional motility experiment, where the head of the filament is spatially fixed. We present a simple phenomenological dynamical model that exhibits both the rotation and the oscillation of the filament as symmetry breaking instabilities of the filament conformation under pertinent boundary conditions.

PACS numbers: 87.45.–k, 02.30.Jr, 87.22.Jb

From the viewpoint of nonequilibrium dynamics, there are many biological systems of interest which fall into the category of *systems of coupled active elements*. For systems of this type, the origin of nonequilibrium motion is built into each of these elements, but the coupled nature of the system often gives rise to new dynamical behavior which is not inherent in the individual elements.

In this Letter we consider as a representative of such systems a system consisting of a filament (either actin or microtubule) and many motor proteins (myosin, kinesin, or dynein) in the presence of an ATP solution. Many experiments have been done on this system using an *in vitro* setup [1], where the protein motors are firmly attached on the surface of a glass plate. These motors cause a directed sliding motion of the filaments with which they come into contact. Although the actual active elements are the protein motors, it suffices for our purpose that we regard a filament as a continuous train of (effective) active elements, each of which tends to move along the tangential direction of the filament.

We shall focus on one phenomenon which is observed in the *in vitro* setup, but does not usually occur in actual *in vivo* biological systems. Here, the head of the filament is somehow pinned at a point on the glass plate, and the filament exhibits either rotation or flapping oscillation [Figs.1(a) and 1(b)]. Our qualitative picture of this phenomenon is the following. (i) The driving force exerted by the active elements is accumulated along the filament, inducing a buckling instability of the otherwise straight filament [2]. (ii) The filament is thus bent, and a part of the motile force acts to displace the filament around the head. (iii) Different types of motion of the filament stem from different types of boundary conditions. Experimentally [3], a rotational motion is observed when the head of the filament is pinned down on the substrate and is free to rotate. We shall call the head in this case a *torque-free head*. On the other hand, a flapping motion is seen when the filament is pinned a short distance from the head, at the "neck." The portion ahead of the pinned site is stretched, maintaining its orientation [4]. Hereafter, for simplicity we shall call this pinned neck the *oriented head* and ignore the portion ahead of the pinned point.

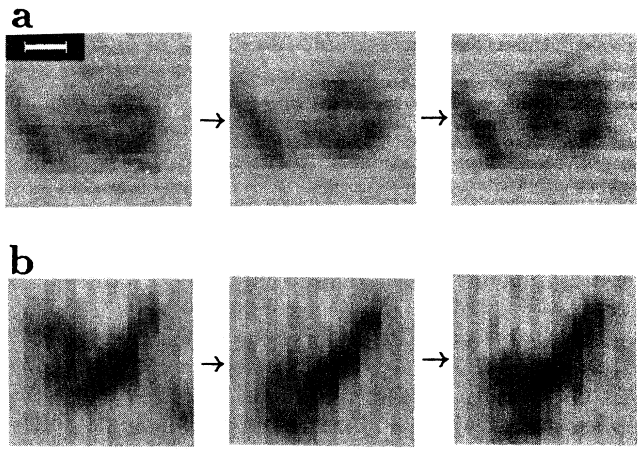

FIG. 1. Consecutive video images of the *in vitro* motility experiment [3]: The pinned actin filaments (thick dark curve) undergo either rotation [series (a)] or flapping oscillation [series (b)]. The time intervals between consecutive images are (a): 0.2 sec and (b): 0.4 sec. The white bar corresponds to 1 μm. In series (b), a part of the filament is ahead of the pinned point and is stretched (the upper right portion). This portion fixes the tangential direction at the pinned point of the filament.

 0031-9007/95/75(1)/172(4)$06.00

We should note that in referring to the two-dimensional nature of the present system we are *not* referring to the background on which active elements are arrayed and mutually coupled, but rather to the spatial degrees of freedom assigned to each of these elements along the filament. In this context it is interesting to relate the spatial symmetry breaking of the system to the instabilities corresponding to Figs. 1(a) and 1(b). First, in the case of a torque-free head, the state of a straight filament with a specific orientation already breaks the orientational symmetry of the system. This implies the existence of a Goldstone mode in the linear stability analysis around the state of a straight filament. We fix the orientation of the reference straight filament either by arbitrarily choosing the "phase angle" (in the case of a torque-free head) or by aligning along the orientation of the head (in the case of an oriented head). There still remains the mirror symmetry with respect to the line defined by the straight filament. This symmetry is finally broken by the buckling mentioned above. As we will show later, the presence of the Goldstone mode in the case of a torque-free head leads to an (nonaccidental) instability of codimension 2 [5].

Our phenomenological model based on the picture described above consists of three simple ingredients: the bending rigidity of the filament, the passive friction between the filament and substrate, and the active motile force working along the filament. We will show that, in our model, both types of motion depicted in Fig.1 are evidently inferred from the linear instability of the steady state of a straight filament [6].

We describe by $\vec{r}\,(s,t)$, with $0 \le s \le \ell$, the conformation of a filament at time t. The argument s is the material coordinate defined as the arc length measured from the tail when the filament is free from stress. The bound ℓ is thus the natural length of the filament. We denote by $\hat{\tau}(s,t)$ the unit tangent vector of the filament at $\vec{r}\,(s,t)$, i.e., $\hat{\tau} = |\vec{r}\,'|^{-1}\vec{r}\,'$, where $\vec{r}\,' \equiv \partial\vec{r}/\partial s$. Ignoring the inertia effect, we propose the following equation of motion:

$$(\zeta_\parallel \hat{\tau}\hat{\tau} + \zeta_\perp[\mathbf{1} - \hat{\tau}\hat{\tau}]) \cdot \frac{\partial \vec{r}}{\partial t} = -\frac{\delta(H_B + H_E)}{\delta \vec{r}} + f_0\hat{\tau}, \qquad (1)$$

where $\mathbf{1}$ is the unit 2×2 matrix, and $\hat{\tau}\hat{\tau}$ is a dyadic. The left-hand side of (1) is the frictional force with the phenomenological friction constants $\zeta_\parallel$ and $\zeta_\perp$ corresponding to longitudinal and transversal sliding motion, respectively. The frictional force originates from the repetitive attachment-detachment processes of protein motors with the filament [7]. The first term on the right-hand side represents the elastic forces in the filament, where H_B is the bending energy [$H_B = (B/2)\int_0^\ell ds|\partial\hat{\tau}/\partial s|^2$ with a bending modulus B (>0)], and H_E is the longitudinal compression energy [$H_E = (E/8)\int_0^\ell ds\,(|\vec{r}\,'|^2 - 1)^2$ with E (>0) being Hooke's constant]. We will eventually take the limit of incompressibility, $E \longrightarrow \infty$, in which the longitudinal stress $\sigma_\parallel$ defined by $\partial(\sigma_\parallel\hat{\tau})/\partial s = -\delta H_E/\delta\vec{r}$ becomes an equivalent of the Lagrange multiplier corresponding to the incompressibility constraint. The detailed form of H_E is, therefore, unimportant. It is only important that it prefers the stress-free state $|\vec{r}\,'| = 1$. In the last term on the right-hand side, f_0 (>0) denotes the motile force along the filament [$\|\hat{\tau}(s,t)$] directed toward the head ($s = \ell$). The velocity dependence of the motile force is ignored for simplicity. That this force is directed along $\hat{\tau}$ is a plausible but unproven assumption. It is at least consistent with experimental data (see discussion in the concluding paragraph).

The boundary condition at the tail ($s = 0$) results from the requirement that the variation $\delta(H_B + H_E)$ vanishes with respect to both the translational variation $\delta\vec{r}\,(0,t)$ and the orientational variation $\delta\hat{\tau}(0,t)$. This boundary condition can be shown to become $|\vec{r}\,'(0,t)| = 1$ and $(\mathbf{1} - \hat{\tau}\hat{\tau}) \cdot \partial^2\hat{\tau}/\partial s^2 = \partial\hat{\tau}/\partial s = 0$. We assume that the (pinned) head is at the origin $\vec{r}(\ell,t) \equiv \vec{0}$. For the torque-free head, we require $(\mathbf{1} - \hat{\tau}\hat{\tau}) \cdot \partial^2\hat{\tau}/\partial s^2 = \vec{0}$ at $s = \ell$, while for the oriented head we assume that the head is oriented in the positive x direction; $\hat{\tau}(\ell,t) = (1,0)$ in Cartesian coordinates.

Next, we introduce the straight steady state for which we analyze the linear stability. We assume that in the steady state the filament lies along the negative x axis as $\vec{r}(s,t) = (r_0(s),0)$, with $r_0(\ell) = 0$. The filament is compressed from its natural length by the motile force, that is, $-\ell \le r_0(0) < 0$. We can derive the expansion of $r_0'(s)$ in terms of $1/E$ as $r_0'(s) = 1 - E^{-1}f_0 s + O(E^{-2})$, for $0 \le s \le \ell$. In order to obtain the linearized equations of motion, we substitute the expression $\vec{r}(s,t) = (r_0(s),0) + (u_\parallel(s,t), u_\perp(s,t))$ into (1) as well as into the pertinent boundary conditions. Up to $O(u_\perp)$ we obtain in the $E \longrightarrow \infty$ limit [8]

$$\zeta_\perp \frac{\partial u_\perp}{\partial t} = -B\frac{\partial^4 u_\perp}{\partial s^4} - f_0 s\frac{\partial^2 u_\perp}{\partial s^2}, \quad 0 < s < \ell, \qquad (2)$$

together with the boundary condition either

$$\left.\frac{\partial^2 u_\perp}{\partial s^2}\right|_{s=0} = \left.\frac{\partial^3 u_\perp}{\partial s^3}\right|_{s=0} = u_\perp(\ell,t) = \left.\frac{\partial^2 u_\perp}{\partial s^2}\right|_{s=\ell} = 0 \qquad (3)$$

for the torque-free head, or

$$\left.\frac{\partial^2 u_\perp}{\partial s^2}\right|_{s=0} = \left.\frac{\partial^3 u_\perp}{\partial s^3}\right|_{s=0} = u_\perp(\ell,t) = \left.\frac{\partial u_\perp}{\partial s}\right|_{s=\ell} = 0 \qquad (4)$$

for the oriented head. For $u_\parallel$ we have the following simple diffusion equation: $\zeta_\parallel(\partial/\partial t)u_\parallel = E(\partial^2/\partial s^2)u_\parallel + O(E^0)$. This equation is irrelevant to the present stability analysis. The factor $f_0 s$ on the right-hand side of (2) reflects the fact that the destabilizing tendency is enhanced near the pinned head, where compressive stress is the largest. If we were to remove the s dependence introduced by this term, (2) would reduce to the usual

equation encountered in the buckling problem of rods in a viscous background [2].

By writing $u_\perp(s,t) = \exp[\Lambda(t/\tau)]\ \psi(s/\ell)$ with $\tau \equiv \zeta_\perp \ell^4/B$, the stability problem is reduced to the following eigenvalue problem: $\Lambda\psi(x) = -\psi''''(x) - \mu x\psi''(x)$ for $0 < x < 1$, where $\psi''(x) \equiv \partial^2\psi(x)/\partial x^2$, etc., and $\mu \equiv f_0\ell^3/B$ is the single dimensionless parameter of the model in the limit $E \longrightarrow \infty$.

In the case of the torque-free head, we have from (3) $\psi''(0) = \psi'''(0) = \psi(1) = \psi''(1) = 0$. There always exists a zero eigenvalue $\Lambda_0 = 0$ of the above equation corresponding to the Goldstone mode $\psi_0(x) = x - 1$. With this exception, all the eigenvalues are negative for $\mu < \mu_c^{\rm rot} \simeq 30.6$. As μ is increased beyond $\mu_c^{\rm rot}$, a single eigenvalue becomes a real positive number. We can prove, however, that at $\mu = \mu_c^{\rm rot}$ the only nontrivial solution of the equation $0 = -\psi''''(x) - \mu_c^{\rm rot} x\psi''(x)$ is $\propto \psi_0(x)$ [9]. According to the theory of linear algebra, this implies that there exists a function $\phi_0(x)$ which, together with $\psi_0(x)$, defines a so-called generalized eigenspace of the eigenvalue Λ_0 $(= 0)$ at the threshold $\mu = \mu_c^{\rm rot}$. $\phi_0(x)$ must satisfy $-\phi_0'''' - \mu_c^{\rm rot} x\phi_0''(x) \equiv \psi_0(x)$ for $0 < x < 1$ under the boundary condition $\phi_0''(0) = \phi_0'''(0) = \phi_0(1) = \phi_0''(1) = 0$. Using the formal power series expansion $\phi_0(x) = \sum_{n=0}^{\infty} c_n x^n$, we can obtain implicit but analytical expressions for $\mu_c^{\rm rot}$ and $\phi_0(x)$. The inset of Fig. 2 shows the forms of $\phi_0(x)$ and $\psi_0(x)$. In particular, the value of $\mu_c^{\rm rot}$ is shown to be a real positive root of the following equation of μ: $\sum_{p=0}^{\infty} (-1)^{p-1}[(3p+3)!]^{-1} \times[3^{p+1}(p+1)! - \prod_{k=0}^{p}\{3(p-k)+1\}]\mu^p = 0$.

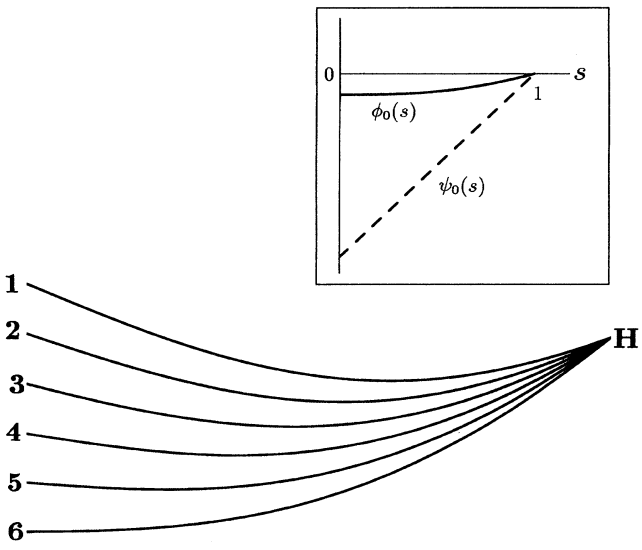

FIG. 2. The rotation of the filament (the solid curves) is constructed from the functions $\psi_0(s)$ and $\phi_0(s)$ (see inset) representing the marginal modes at the instability threshold of the system with a torque-free head (marked by H). The time increases from 1 to 6 with the interval 0.09τ ($\tau \equiv \zeta_\perp\ell^4/B$).

We can infer the behavior of $u_\perp(s,t)$ slightly beyond the threshold $\mu \gtrsim \mu_c^{\rm rot}$ by ignoring all the fast-decaying modes. Putting $u_\perp(s,t) = u_0(t)\psi_0(s/\ell) + v_0(t)\phi_0(s/\ell)$, we propose the following weakly nonlinear equation for small t/τ:

$$\tau\frac{\partial}{\partial t}\begin{bmatrix} u_0 \\ v_0 \end{bmatrix} = \begin{bmatrix} 0 & 1 \\ 0 & \epsilon \end{bmatrix}\begin{bmatrix} u_0 \\ v_0 \end{bmatrix} - \beta\begin{bmatrix} 0 \\ v_0^3 \end{bmatrix}, \qquad (5)$$

where $\epsilon \propto \mu - \mu_0^{\rm rot}$ and $\beta(>0)$ is a constant. The linear terms in (5) come from the linear analysis, while the lowest order nonlinear term is constructed so as to satisfy the symmetry properties of the fully nonlinear equation (1) [10]. Equation (5) has a solution $u_\perp(s,t) = (\epsilon/\beta)^{1/2}[(t/\tau)\psi_0(s/\ell) + \phi_0(s/\ell)]$. Figure2 shows the motion of the filament described by this expression. Although the rotational symmetry is not fully retained in (5), this solution implies that the filament rotates around the fixed head at an angular velocity $(\epsilon/\beta)^{1/2}/\tau$ without changing its shape ϕ_0. The overall amplitude $(\epsilon/\beta)^{1/2}$ is somewhat exaggerated in the figure.

In the case of an oriented head, (4) implies the boundary conditions $\psi''(0) = \psi'''(0) = \psi(1) = \psi'(1) = 0$ for the eigenvalue equation appearing above. We found that in this case a Hopf-type instability occurs at $\mu = \mu_c^{\rm osc} \simeq 75.5$. The threshold eigenvalues are $\Lambda = \pm\Omega_c i$, with $\Omega_c \simeq 193.1$. These numerical values can be obtained by solving the discretized version of the eigenvalue problem. At the threshold, the critical eigenfunctions are a pair of complex conjugate functions, which we denote $\psi_H(x)$ and $\psi_H^*(x)$. In the inset of Fig.3 we show the profiles of the real part $\mathrm{Re}(\psi_H)$ and of the imaginary part $\mathrm{Im}(\psi_H)$. Taking account of only these slow modes for $\mu \gtrsim \mu_c^{\rm osc}$, we assume the expression $u_\perp(s,t) = u_H(t)\psi_H(s/\ell) + u_H(t)^*\psi_H^*(s/\ell)$ and propose the following weakly nonlinear equation:

$$\tau\frac{\partial}{\partial t}\begin{bmatrix} u_H \\ u_H^* \end{bmatrix} = \begin{bmatrix} \tilde\epsilon + i\Omega_c & 0 \\ 0 & \tilde\epsilon - i\Omega_c \end{bmatrix}\begin{bmatrix} u_H \\ u_H^* \end{bmatrix} - \tilde\beta\begin{bmatrix} |u_H|^2 u_H \\ |u_H|^2 u_H^* \end{bmatrix}, \qquad (6)$$

where $\tilde\epsilon \propto \mu - \mu_c^{\rm osc}$ and $\tilde\beta$ (>0) is again a constant. Equation (6) has the oscillatory solution $u_H(t) = (\tilde\epsilon/\tilde\beta)^{1/2}e^{i\Omega_c t/\tau}$. The time evolution of $2\,\mathrm{Re}[u_H(t)\psi_H(s/\ell)]$ obtained from this equation is shown in Fig. 3. The magnitude of $\tilde\epsilon/\tilde\beta$ is again somewhat exaggerated. This weakly nonlinear solution exhibits the essential feature of the observed flapping oscillation [see Fig. 1(b)].

Before discussing what our theory can contribute to the knowledge of biophysical systems, we should note that the oscillatory instability in the case of a torque-free head is that related to the so-called codimension-2 bifurcation [5]. In order to see this, we have reexamined the above equation $\Lambda\psi(x) = -\psi''''(x) - \mu x\psi''(x)$ for $0 < x < 1$ using the slightly generalized boundary condition $\psi''(1) +$

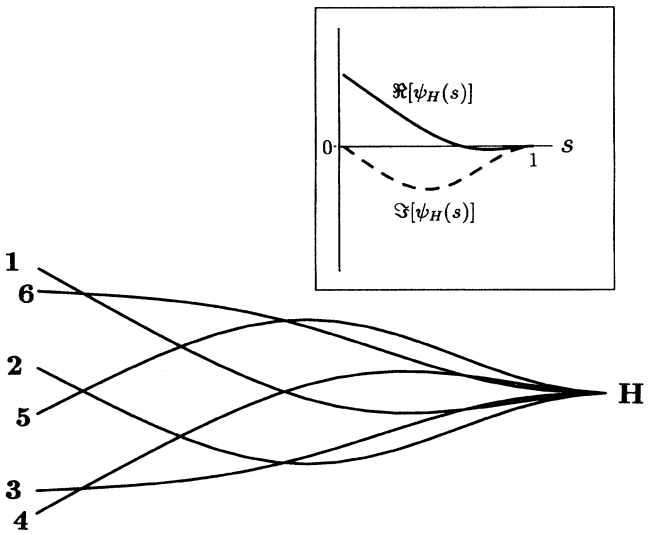

FIG. 3. The flapping oscillation of the filament (solid curves) is constructed from the functions $\mathrm{Re}[\psi_H(s)]$ and $\mathrm{Im}[\psi_H(s)]$ (see inset) representing the marginal modes at the Hopf-type instability threshold of the system with an oriented head (marked by H). The time increases from 1 to 6 (and then to 1) with the interval 1/6 of the period of oscillation, $2\pi\tau/\Omega_c$ ($\Omega_c \simeq 193.1$).

$\kappa\psi'(1) = 0$ in place of either the condition $\psi''(1) = 0$ (i.e., $\kappa = 0$) or $\psi'(1) = 0$ (i.e., $\kappa = \infty$) used in the above analysis. Physically, this condition corresponds to a head with an "elastic hinge" and may be more close to the reality of Fig. 1(b). Using a numerical diagonalization technique, we found that, for $\kappa \longrightarrow 0$ and for $\epsilon \propto \mu - \mu_c^{\mathrm{rot}} \longrightarrow 0$, the two relevant eigenvalues corresponding to the slowest modes are asymptotically given as the roots of the equation $\Lambda^2 + (C_1\epsilon - C_2\kappa)\Lambda + C_2\kappa = 0$, where C_1, C_2, and C_3 are positive real constants. Only when $\kappa = 0$ does the Goldstone mode ($\Lambda = 0$) exist. For $\kappa > 0$ the Hopf-type instability occurs at $\epsilon = C_1^{-1}C_2\kappa$ [5].

Next, we try to assess the magnitude of the phenomenological friction constants $\zeta_\parallel$ and $\zeta_\perp$ using the results of our analysis. These friction constants are of biophysical interest since they reflect the parameters concerning the interaction processes between protein motors and filaments [7]. In our theory the rotation of the filament occurs for $\mu \equiv f_0\ell^3/B \gtrsim 30.6$. Adopting the estimate $B \simeq (2 - 3) \times 10^{-17}$ dyn cm^2 [11] for an actin filament and also using the value $\ell \simeq 4$ μm taken from the experimental observation shown in Figs. 1(a) and 1(b), we deduce f_0 to be bounded from below as $f_0 \geq f_{0\min} \simeq (1-1.5) \times 10^{-5}$ dyn/cm. On the other hand, from our phenomenological model the sliding velocity $v_\parallel$ of a straight filament without pinning is $v_\parallel = f_0/\zeta_\parallel \geq f_{0\min}/\zeta_\parallel$. From the experimentally observed value of $v \simeq 5$ μm/sec, we therefore have $\zeta_\parallel \geq f_{0\min}/v_\parallel \simeq (2-3) \times 10^{-2}$ dyn sec/cm^2. With regard to the flapping oscillation, the angular frequency at the threshold, ω_c^{osc}, is given by $\Omega_c/\tau = 193.1B/(\zeta_\perp\ell^4) \simeq (1.5-2) \times 10^{-1}\zeta_\perp^{-1}$ sec^{-1}. Since we have no data for ω_c^{osc}, we adopt as a tentative estimate the experimentally observed angular frequency of flapping motion, ~ 5 sec^{-1}, beyond the instability threshold. We thus have a rough estimate of $\zeta_\perp \simeq (3-5) \times 10^{-2}$ dyn sec/cm^2. It may not be counterintuitive to assume here that $\zeta_\perp$ is larger than $\zeta_\parallel$. Then our crude estimation leads to the following interesting conclusion: $\zeta_\parallel \simeq \zeta_\perp$ for the *in vitro* experiments. This conclusion implies that, in the absence of pinning, strongly anisotropic, that is, quasi-one-dimensional, sliding motion of the filaments is controlled not by the anisotropic friction, but by the motile force which each protein motor *knows* to exert along the filament. We also note the simulation of (1) with $\zeta_\parallel = \zeta_\perp$ reproduces the observed *in vitro* motion of the filament quite well [6].

One of the authors (K.S.) is grateful to H. Kozono, L. Leibler, A. Ott, J. Prost, and J.-L. Viovy for fruitful discussions. We thank Y. Imafuku for helping with the image analysis of the experimental data. This work is supported in part by Grants-in-Aid for Scientific Research (No. 0564022 and No. 0460150) to K.S., and by a Grant for the Joint Research on the *in vitro* sliding movement to K.T. and K.S., from the Ministry of Education, Science and Culture of Japan.

[1] S. J. Kron and J. A. Spudich, Proc. Natl. Acad. Sci. U.S.A. **83**, 6272 (1986).
[2] L. D. Landau and E. M. Lifshitz, *Theory of Elasticity* (Pergamon, New York, 1973), Chap. 20.
[3] Y. Y. Toyoshima (unpublished).
[4] Usually the pinning is not perpetual, and sometimes the crossover from the rotational motion to the flapping oscillation is observed within a single filament.
[5] J. Guckenheimer, *Nonlinear Oscillations, Dynamical Systems, and Bifurcations at Vector Fields* (Springer-Verlag, New York, 1990), 3rd ed., Chap. 7.
[6] The numerical simulation of the full nonlinear model will be reported elsewhere; N. Mori and K. Sekimoto (to be published).
[7] K. Tawada and K. Sekimoto, J. Theor. Biol. **150**, 193 (1991); K. Sekimoto and K. Tawada (to be published).
[8] In deriving (2) we need the expansion of $r_0'(s)$ up to $O(E^{-1})$ order.
[9] M. Abramowitz and I. A. Stegun, *Handbook of Mathematical Functions* (Dover, New York, 1964), p. 466.
[10] Logically a bifurcation of the subcritical type is also possible. But the essential features of the solution in the weakly nonlinear regime will be the same, as inferred from the preliminary full nonlinear analysis [6].
[11] S. Fujime, S. Yoshino, and Y. Umazume, in *Cross-Bridge Mechanism in Muscle Contraction*, edited by H. Sugi and H. Pollack (University of Tokyo, Tokyo, 1979), p. 51.

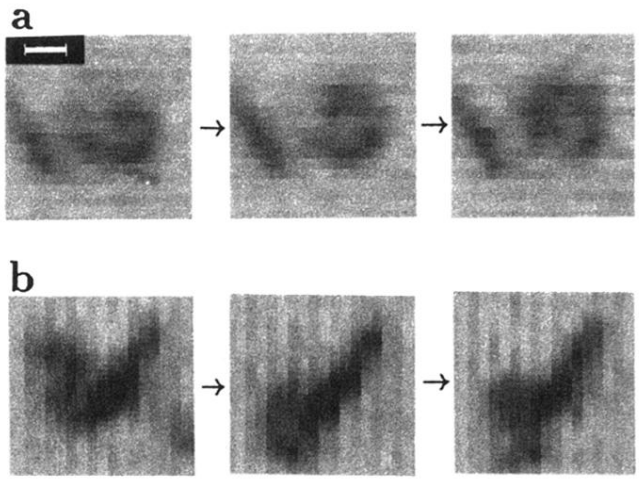

FIG. 1. Consecutive video images of the *in vitro* motility experiment [3]: The pinned actin filaments (thick dark curve) undergo either rotation [series (a)] or flapping oscillation [series (b)]. The time intervals between consecutive images are (a): 0.2 sec and (b): 0.4 sec. The white bar corresponds to 1 μm. In series (b), a part of the filament is ahead of the pinned point and is stretched (the upper right portion). This portion fixes the tangential direction at the pinned point of the filament.